# Unravelling the band crossings in $^{68}$Se and $^{72}$Kr: The quest for $T=0$ pairing

S. M. Fischer
*Department of Physics, DePaul University, Chicago, Illinois 60614, USA*
*and Physics Division, Argonne National Laboratory, Argonne, Illinois 60439, USA*

C. J. Lister
*Physics Division, Argonne National Laboratory, Argonne, Illinois 60439, USA*

D. P. Balamuth
*Department of Physics and Astronomy, University of Pennsylvania, Philadelphia, Pennsylvania 19104, USA*
(Received 13 March 2003; published 27 June 2003)

High-spin band crossings in $N=Z$ nuclei have been suggested to contain information on $T=0$ neutron-proton pairing correlations. Several experiments that produced high angular momentum states in the $N=Z$ nuclei $^{68}_{34}$Se and $^{72}_{36}$Kr have been carried out. Levels in these neutron deficient nuclei were populated through heavy-ion fusion reactions and their subsequent $\gamma$ decay was measured with Gammasphere. The combination of these data allowed the level sequence in yrast and near yrast bands to be firmly established, extended to higher spin, and has resolved some previously published discrepancies. The yrast sequence in $^{68}$Se was extended to spin $J=26$ and a new band crossing observed. In $^{72}$Kr, the ground state band was found to fork into three bands, each of which has irregularities in its moment of inertia. Differential Doppler shift measurements indicate that the two high-spin bands have very different shapes. Similar, sharp band crossings were established in both nuclei. A comparison of these data with recent measurements of $N=Z+2$ nuclei $^{70}$Se and $^{74}$Kr allowed the issue of ‘‘delayed alignments’’ to be addressed in detail. No clear-cut evidence for any delay was found.

DOI: 10.1103/PhysRevC.67.064318 PACS number(s): 21.10.−k, 23.20.En, 23.20.Lv, 27.50.+e

## I. INTRODUCTION

The alignments and backbends of rotational sequences in even-even intermediate mass $N=Z$ nuclei have been the focus of intense theoretical [1–9] and experimental [10–15] scrutiny. The main reason for this attention is the notion that neutron-proton ($np$) pairing modes, either with $T=0$ or 1, could augment the normal $T=1$ neutron and proton pairing fields and modify high-spin behavior, particularly altering the nuclear moment of inertia at high spin. Specifically, it has been suggested that pair fields with $T=0$ isospin symmetry would respond less abruptly to the Coriolis interaction associated with rotation and cause delays in the pair breaking, or alignment frequencies at which the nucleus begins a transition from superfluid to rigid body behavior. These changes in the moment of inertia can be inferred by measuring the $\gamma$ rays emitted as the nucleus cools and slows in its rotation. As there are few other clear-cut experimental signatures presently available to probe these short-range $np$ correlations, this line of research has been very active.

Unfortunately, a clear understanding of these alignments has been very slow in coming, both in the theoretical and experimental domains. In theory, the difficulties arise as the pairing fields are intimately connected with the shape of the nucleus, as are the exact locations of single particle states near the Fermi surface. Rigorously associating shifts in alignment frequency with $np$ pairing correlations alone, and not with effects arising from the shape degrees of freedom, has been elusive. Schematic calculations including $np$ pairing interactions have been made for the $A\sim 70$–80 region, but the full $fpg$-shell model space is too large to permit exact shell model calculations, so various approximations have to be made which further cloud the issues. In experiment, the key nuclei lie far from stability, and the total production cross sections of individual isotopes are very small ($\sim 200$ $\mu$b). Performing detailed spectroscopy above spin $J=14$, where the interesting physics occurs, is at the limits of current experimental techniques, even using the largest detector arrays. As we will discuss, the experimental situation in $^{68}$Se and $^{72}$Kr is further exacerbated by oblate-prolate shape coexistence and a very unusual ‘‘forking’’ in $^{72}$Kr.

The central issue of an ‘‘alignment delay’’ in rotational frequency caused by $np$ pairing focuses on identifying a reference that constitutes normal behavior, or no delay. In heavy nuclear rotors like those found in the rare-earth and actinide regions, the nuclear shape is very stable and neighboring nuclei can provide this reference. In the intermediate mass nuclei under discussion, this assumption is not valid as the nuclei change in shape when the neutron or proton number, or even the rotational frequency, is varied. Consequently, the interpretation of an experimentally observed delay is always far from clear. There is theoretical consensus [16–19] that the $T=0$ component of the $np$ correlation should be strongly favored in $N=Z$ nuclei, and rapidly fall when $N>Z$ to a point that it is rather insignificant in stable heavy nuclei. As a result, the search for $T=0$ correlations has centered around comparing alignments in $N=Z$ and $N=Z+2$ isotopes in nuclei that are heavy enough to support the notion of a pairing field.

Another area of emerging consensus [20–23] is the inference that although $np$ correlations, in general, are important in determining the ground state binding energy, pair transfer

 

TABLE I. Description of the experimental datasets used in this work. "GS ID" refers to the identification number of the Gammasphere experiment.

| Reaction | $E_{beam}$ (MeV) | GS ID | Location | Auxiliary detectors |
|---|---|---|---|---|
| $^{36}$Ar+$^{40}$Ca | 145 | GS52 | 88-Inch Cyclotron | Microball, Neutron detectors[a] |
| $^{40}$Ca+$^{40}$Ca | 160 | GSFMA19 | ATLAS | Microball, Neutron detectors[b] |
| $^{58}$Ni+$^{12}$C | 220 | GSFMA32 | ATLAS | FMA |
| $^{36}$Ar+$^{40}$Ca | 145 | GSFMA74 | ATLAS | Microball, Neutron shell[c] |

[a]15 scintillators from the University of Pennsylvania and the University of Manchester.
[b]20 scintillators from the University of Pennsylvania and the University of Manchester.
[c]The 30 detector neutron shell from Washington University.

'cross sections, and low spin properties of both even-even and odd-odd $N=Z$ nuclei, the $T=0$ $np$ contributions appear weak relative to $T=1$ contributions. Couplings with $T=1$ and higher order ($\alpha$-like clustering) are dominant. What is much more controversial is how these correlations are diminished with spin. It has been suggested that the experimental observations can be explained by $T=1$ pairing alone [3], or require enhanced $T=1$ correlations that might simulate the effect of $T=0$ pairs [4], or that there is a switch from $T=1$ to $T=0$ pairing with increasing spin [5]. It is this area that is the focus of the present research: an attempt to improve the experimental data to allow these questions to be more rigorously challenged.

In this paper we have solidified the experimental situation in the $N=Z$ nuclei $^{68}$Se and $^{72}$Kr and compared these data to neighboring nuclei in a manner that helps to clarify the cause of the irregularities in the moments of inertia. The evidence for alignment delay and its possible implications are then considered.

## II. THE EXPERIMENTS

All the experiments were heavy-ion fusion evaporation studies, carried out either at the 88-Inch cyclotron at Berkeley or at the ATLAS linear accelerator at Argonne. In all cases the $\gamma$ rays were detected using Gammasphere [24], the U.S. national $\gamma$-ray facility. In these experiments, it was configured with either ~70 or ~100 Compton suppressed, large volume germanium detectors, with channel selection through light charged particle [25] and neutron detection, or by detecting reaction products in the Argonne Fragment Mass Analyzer (FMA) [26]. Table I summarizes the experiments, including details of the reactions, Gammasphere configuration, and channel selection mode.

## III. ANALYSIS

This paper presents a careful comparative analysis of several datasets in order to clarify the band structures in $^{68}$Se and $^{72}$Kr. No single reaction or single beam energy contains sufficient information to allow the construction of unambiguous $\gamma$-ray decay schemes. This is particularly true for establishing the sequence of $\gamma$ rays in a single, long deexcitation cascade. Population at low beam energies allows the low-lying sequence to be established and ordered, as the intensity drops off quickly with spin, while population at higher beam energies allows the cascades to be extended to the highest angular momenta.

### A. $^{68}$Se

In $^{68}$Se, a recent low spin study [27] extended previous work [28,29] and allowed an investigation of oblate-prolate shape coexistence. $^{68}$Se has emerged as one of the few nuclei in nature with a substantial oblate ground state deformation. However, the small moment of inertia of the oblate configuration leads to near-prolate states becoming yrast above $J=6$. In the current analysis, the yrast line was extended from $J=12$ to $J=26$. This was quite difficult, as in two places there are backbends, and both irregularities occur at closely spaced energies (1161/1047 keV and 1169/1048 keV). These doublets could only be deconvoluted through comparison of datasets; the Ni+C reaction only populated the lower doublet, while the high-spin experiments populated both. The left panel of Fig. 1 shows the resulting decay scheme for $^{68}$Se, and Table II includes information on transition energies and intensities deduced from the $^{36}$Ar+$^{40}$Ca reaction. The quality of the data can be seen in Fig. 2, which shows a composite spectrum of $\gamma$ rays in $^{68}$Se produced from a sum of $\gamma\gamma$-gated channel-subtracted coincidence spectra. The 1048-keV member of the 1047/1048-keV doublet can be isolated by requiring that the transition be in coincidence with the 1362-keV and 1449-keV transitions, as shown in Fig. 3.

Angular distributions were analyzed in order to determine the multipolarity of transitions. Due to the small cross section for this reaction, data for the individual Gammasphere rings were grouped into five sets of angles. A "channel subtraction," which consisted of removing the background due to the feedthrough of reaction channels with higher particle multiplicity, was performed, and single $\gamma$-ray gates over all angles on the known transitions in $^{68}$Se were applied. Sample data are shown in Fig. 4 for the 1449-keV $8^+\rightarrow 6^+$ transition between the prolate and oblate states (upper panel), and for the newly observed 1169-keV $18^+\rightarrow 16^+$ transition. Both distributions are consistent with $L=2$ multipolarity. The results of this analysis are included in Table II. Above spin $J=18$, the transitions are too low in intensity to extract individual angular distributions. However, above this point the band spacings become regular and appear consistent with a rotational cascade of $E2$ transitions.

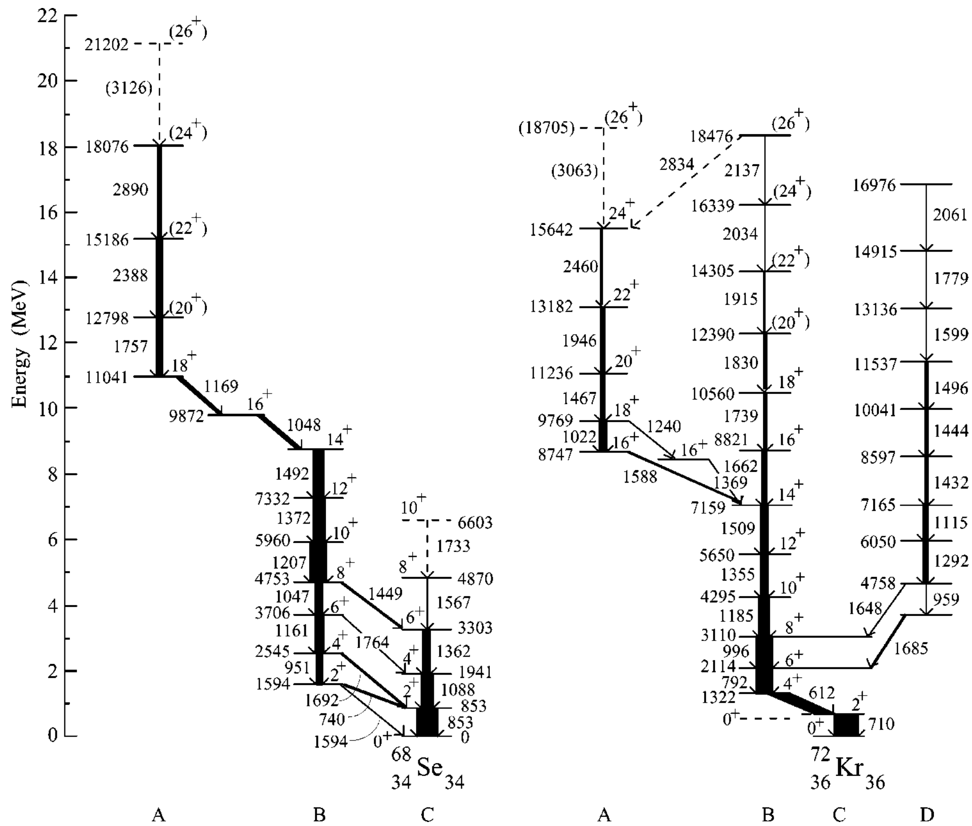


FIG. 1. The decay schemes for $^{68}$Se and $^{72}$Kr deduced from this work. The $^{68}$Se sequences were inferred from the $^{12}$C($^{58}$Ni,$2n$) and $^{40}$Ca($^{36}$Ar,$2\alpha$) reactions, and the $^{72}$Kr sequences from the $^{40}$Ca($^{40}$Ca,$2\alpha$) reaction.

### B. $^{72}$Kr

The lowest excited states in $^{72}$Kr were observed in 1987 by Varley *et al.* [30] in an elegant experiment that used the Daresbury recoil separator to identify recoiling krypton nuclei that were produced in the highly inverse reaction $^{58}$Ni $+^{16}$O at 170 MeV. Six candidate transitions were identified as belonging to $^{72}$Kr from the recoil-gated $\gamma$-ray singles data. Although spins were not assigned, the lowest three transitions in the ground state band were clearly identified (709, 612, and 790 keV). Dejbakhsh *et al.* [31] used $\gamma\gamma$ coincidences and the $^{40}$Ca($^{35}$Cl,$p2n$) reaction at 95 MeV to confirm the lowest two transitions and assigned tentative spins in the ground state band to $J^{\pi}=(8^{+})$.

In 1997, de Angelis *et al.* [10] extended the level scheme significantly to a tentative spin of $16\hbar$ using the GASP array and the $^{40}$Ca($^{40}$Ca,$2\alpha$) reaction at 160 MeV. Transitions in the ground state band were shown to increase regularly in energy in the region between the $4^{+}$ and $14^{+}$ states. A backbend was observed, albeit delayed relative to the frequency predicted by total Routhian surface (TRS) calculations [10], with a 1368-keV $16^{+}\rightarrow14^{+}$ transition placed above the 1509-keV $14^{+}\rightarrow12^{+}$ transition. A deformation of $\beta_2=0.37(7)$ was deduced [10] from a Doppler shift attenuation measurement for the $8^{+}\rightarrow6^{+}$ transition. A parallel study by Hausladen [32], using the $^{40}$Ca($^{36}$Ar,$2p2n$) reaction at 145 MeV and the Gammasphere array, confirmed the ground state band up to a spin of $14\hbar$. This work, however, indicated that the $16^{+}\rightarrow14^{+}$ transition was a 1664-keV transition rather than the 1368-keV $\gamma$ ray observed by de Angelis *et al.* [10]. The result was significant because it implied that the backbend had not been observed, and was delayed to still higher frequency.

Two additional studies were published in 2001, one by Fischer *et al.* [11,14] using the $^{40}$Ca$+^{40}$Ca reaction at 160 MeV, and the other by Kelsall *et al.* [12] using the $^{36}$Ar $+^{40}$Ca reaction at 145 keV. The first reported a smooth continuation of the ground state band to a tentative spin of $26\hbar$, including the 1662-keV transition observed by Hausladen [32], and with no evidence for a backbend at high spin. The 1368-keV transition seen by de Angelis *et al.* [10] was not found to be a continuation of the ground state band. In addition, an irregular sequence that appeared to become yrast was found above spin $12\hbar$; however, it was believed to be associated with a more spherical, terminating configuration rather than a continuation of the ground state band. Kelsall *et al.* [12] confirmed the regular sequence of transitions to spin $20\hbar$. Two transitions (1023 keV and 1588 keV in energy) were tentatively placed as a cascade that fed into the ground state band above spin $12\hbar$, but the linking transitions were not observed. The authors indicated [12] that the 1588-keV transition showed no evidence for a rotational sequence extending to higher energies, similar to the irregular sequence discussed by Fischer *et al.* [14]. The 1367-keV transition observed previously by de Angelis *et al.* [10] was placed as feeding into the 1508-keV $14^{+}\rightarrow12^{+}$ transition, and assigned a tentative spin of $15\hbar$ based on a directional corre-

TABLE II. The energies, spins, and parities of the excited states of $^{68}$Se obtained from the $^{40}$Ca($^{36}$Ar,2$\alpha$) reaction, and the energies, relative intensities, and measured multipolarities of transitions from these states.

| $E_x$ (keV) | $J^\pi$ ($\hbar$) | $E_\gamma$ (keV) | $I_\gamma$ (%) | $L$ ($\hbar$) |
|---|---|---|---|---|
| 853 | $2^+$ | 853.4(2) | | 2 |
| 1594 | $2^+$ | 740(1) | <11 | |
| | | 1594(1) | | |
| 1941 | $4^+$ | 1088.3(2) | 100(15) | 2 |
| 2545 | $4^+$ | 951.1(5) | <12 | |
| | | 1691.7(5) | 53(12) | |
| 3303 | $6^+$ | 1361.5(3) | 71(12) | 2 |
| 3706 | $6^+$ | 1160.7(3) | 46(10) | 2 |
| | | 1764(1) | 34(10) | |
| 4753 | $8^+$ | 1046.7(3) [a] | 44(18) | 2 |
| | | 1448.5(3) | 59(10) | 2 |
| 5960 | $10^+$ | 1207.4(3) | 96(14) | 2 |
| 7332 | $12^+$ | 1372.0(3) [b] | 68(9) | 2 |
| 8824 | $14^+$ | 1491.9(3) [b] | 74(13) | 2 |
| 9872 | $16^+$ | 1047.7(5) | 41(13) | 2 |
| 11 041 | $18^+$ | 1168.6(3) | 46(10) | 2 |
| 12 798 | $(20^+)$ | 1757.1(5) | 17(8) | |
| 15 186 | $(22^+)$ | 2388(2) | 26(16) | |
| 18 076 | $(24^+)$ | 2890(3) | 20(11) | |
| (21 202) | $(26^+)$ | 3126(4) | <10 | |

[a]This transition was fit as a doublet with the transition from the 9872-keV state.

[b]The ordering of these transitions is based on the relative intensities observed in the $^{58}$Ni+$^{12}$C low spin study, which populated states up to spin $J=14$.

lation analysis. Two sidebands were also observed, each feeding into the ground state band at low spin.

The decay scheme for $^{72}$Kr as deduced in this analysis is presented in Table III and the right panel of of Fig. 1, with a composite spectrum of $\gamma$ rays in $^{72}$Kr contained in Fig. 5. The difficulty, contradictions, and confusion in the earlier studies can be understood as the result of an unusual behavior observed around spin 16$\hbar$, where the yrast sequence has a "triple fork," resulting in three $16^+$ states separated by less than 300 keV in energy. The yrast $J=16$ level reported by de Angelis *et al.* [10] in fact carries little flux, and the higher spin configurations decay mainly to the second and third $J=16$ states. The irregular band referred to by Fischer *et al.* [14] and reported by Kelsall *et al.* [12] is now firmly placed and ordered (band A in Fig. 1). Figure 6 shows spectra produced from sums of $\gamma\gamma$ coincidence gates of (upper panel) the 1369-keV transition with members of the ground state band, and (lower panel) the 1467-keV transition with members of the ground state band. From these spectra there is evidence for the placement of the (1240 keV,1369 keV) and (1022 keV,1588 keV) cascades below the 1467-keV $20^+\rightarrow18^+$ transition. Figure 7 shows a sum of $\gamma\gamma$ gates selected to enhance the transitions in band *A*. Placement of the 1588-keV transition below the 1022-keV transition is clear from the measured relative intensities; however, the 1240-keV and 1369-keV intensities are identical. Placement of the 1369-keV transition below the 1240-keV transition is based on the earlier observation of only the 1369-keV $\gamma$ ray by de Angelis *et al.* [10] and Kelsall *et al.* [12]. The poor efficiency for detecting high energy $\gamma$ rays combined with the low statistics for small cross section measurements and the unusual forking behavior observed in this nucleus, make the unravelling of the level scheme difficult. Despite these difficulties, the sequences shown in Fig. 1 are strongly supported by $\gamma$-ray coincidence data and intensity balances. We mention that the $20^+\rightarrow18^+$ 1830-keV transition of band *B* is placed above the 1739-keV $\gamma$ ray, although the measured intensity of the former is greater than (but approximately equal to within errors) that of the latter transition. The ordering of these two transitions is not firm. A search for a 2034-keV transition, which would remove all ambiguity by linking the $J=18$ state of band *B* and the $J=16$ state at 8747 keV, was carried out. If present, such a decay is below our level of sensitivity (five units in Table III).

Angular distributions were analyzed using channel-subtracted spectra on which single $\gamma$-ray gates were applied. The results are included in Table III. The three panels in Fig. 8 present the angular distribution data for the 1588-, 1662-, and 1022-keV transitions in bands *A* and *B*. Each of the distributions is consistent with that expected for quadrupole radiation, supporting the assignment of $J=16$ for the states at 8821 keV and 8747 keV, and the assignment of $J=18$ for the 9769-keV state. Analysis of distributions for the 1369-keV and 1240-keV transitions was not possible due to their low intensity and the presence of a contaminant $\gamma$ ray near 1370 keV.

The high-spin $^{72}$Kr experiment was designed to extend the decay scheme. Thin targets, <500 $\mu$g/cm$^2$, were used to achieve high and uniform recoil velocity and thus minimize the Doppler broadening. However, some sensitivity to nuclear lifetimes remains, specifically for those states that have a high probability of decaying as the nucleus slows down in the target. For $^{72}$Kr recoiling in $^{40}$Ca at ~1 MeV/nucleon this corresponds to states with effective lifetimes (i.e., state lifetime plus feeding time) of 25–100 fs [33]. As shown in Fig. 9, clear differential Doppler effects can be seen when comparing transitions from bands *A* and *B* observed in detectors at forward and backward angles. On average, the transitions in band *B* were emitted from nuclei traveling at a higher velocity than in band *A*, as is clear from the larger Doppler shifts of states near $J=22$. To reliably measure these short lifetimes, the high-spin decay scheme, including detailed information about the feeding, needs to be well known and data of high statistical quality are required in the lifetime region of interest ($J>20$). Further, precise information is required concerning the exact target thickness and composition, the thickness of gold "flashes" on the front and back of the target (which prevent oxidation), and the kinematic bias imposed by detecting evaporated particles. The current experiments were not optimized for such measurements, and the systematic uncertainties have prevented accurate lifetime extraction.

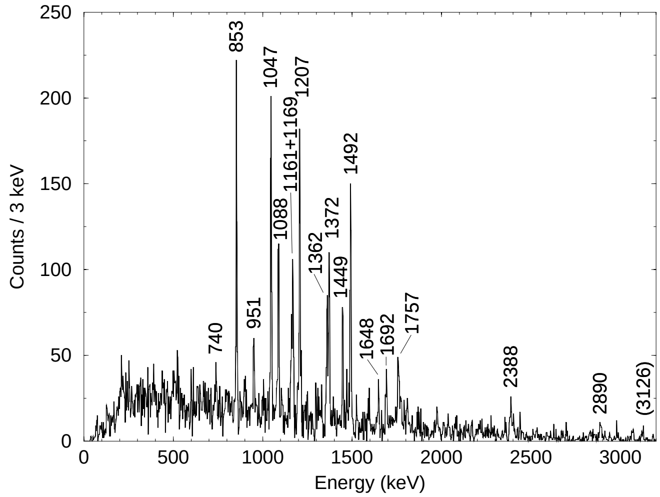


FIG. 2. A spectrum of $\gamma$-ray transitions in $^{68}$Se obtained from a sum of $\gamma\gamma$-gated coincidence spectra. The nucleus was produced in the $^{40}$Ca($^{36}$Ar,2$\alpha$) reaction. Background due to the breakthrough of the $2\alpha 1p$ and $2\alpha 2p$ reaction channels has been subtracted.

What can be more reliably extracted is the lifetime *difference* between the bands, a quantity that is less sensitive to the present uncertainties, as many of the systematic effects cancel. The difference in lifetimes near spin $J=22$ is $\Delta\tau=50(15)$ fs, a result that is found to be rather insensitive to most analysis parameters. At present, only one lifetime is known for $^{72}$Kr [10], the $J=8\rightarrow 6$ ground state band transition, with a mean lifetime of 400(150) fs, corresponding to a transitional quadrupole moment of $Q_t=2.52(47)$ $e$ b. Of the two bands, *A* and *B*, band *B* appears to have the smoothest development of moment of inertia, and corresponds most closely to a rotation without shape change. Assuming a constant quadrupole moment for this band, an extrapolation from spin $J=8$ implies a mean lifetime of 14(5) fs for the $J=22$ state at 14305 keV. As the two bands are close in excitation and are similarly populated, it is quite likely they experience feeding patterns with similar time structure. Under this assumption, we can use the time difference observed for bands *A* and *B* to estimate the mean lifetime of $J=22$ state in band *A* as $14(5)+50(15)=61(16)$ fs. This translates into a quadrupole moment of $Q_t=1.15(15)$ $e$ b, substantially smaller than that of the ground state band. It is this qualitative difference that we will discuss further, though it should be emphasized that a precise investigation of the lifetimes in these bands is very important and is planned. This result is reminiscent of, but more dramatic than, the ‘‘shrinking’’ at high spin reported for $^{74}$Kr [34], where a reduction in the quadrupole moment of $Q_t=2.9$ $e$ b to $Q_t=2.1$ $e$ b was observed.

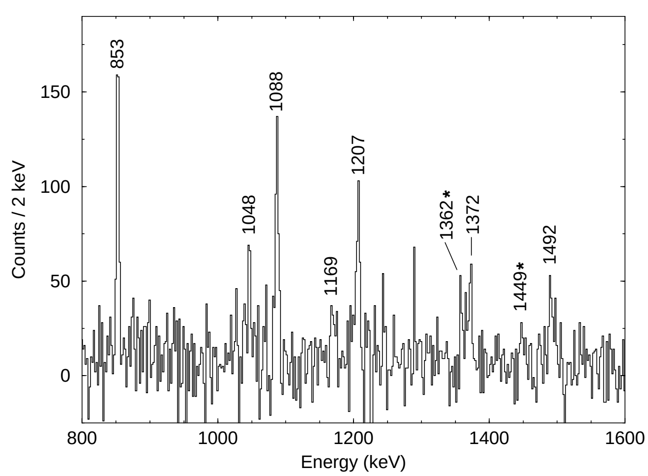


FIG. 3. The sum of single $\gamma$-ray gates on the 1362-keV and 1449-keV transitions in $^{68}$Se. Note the presence of the 1048-keV and 1169-keV transitions and the absence of the 1047-keV and 1161-keV transitions.

Two other rotational structures have been reported [12], decaying into the ground state band at $J=2$ and $J=6$. For the former, we cannot confirm the origin of these transitions, as in our data the band is hardly populated. The higher spin sequence is more strongly populated, but the ordering of transitions is difficult to establish, as many have near-equal intensity. Thus the relative positions of levels in band *D*, shown to the right in Fig. 1, should be viewed as tentative. The final decay scheme inferred from our data sets is now in quite close correspondence with the latest version from the York group [15]. However, the linking transitions we have found at $J=18$ and $J=26$ lift some of the ambiguities inherent in both the decay patterns arising from long cascades of transitions of near-equal intensity.

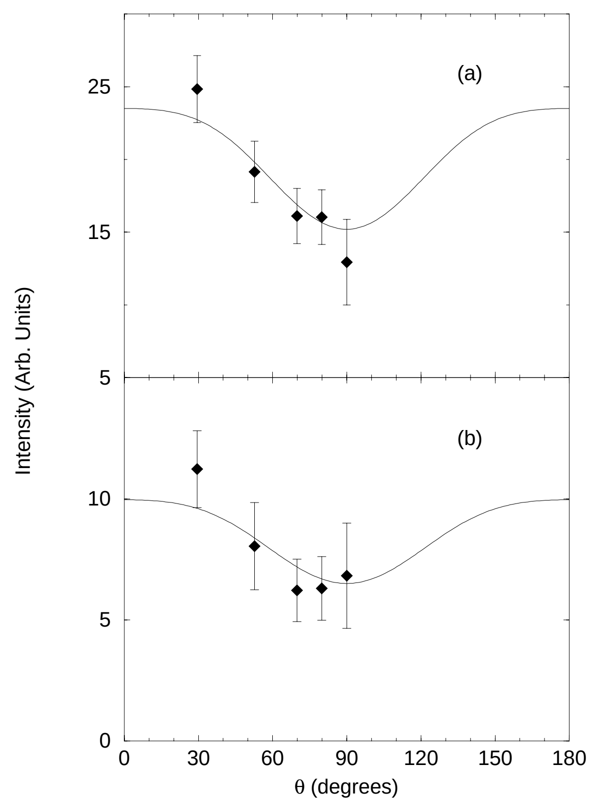


FIG. 4. Angular distribution data for two transitions in $^{68}$Se. The upper panel shows data for the 1449-keV $8^+\rightarrow 6^+$ transition between the prolate and oblate states. The lower panel shows data for the 1169-keV $18^+\rightarrow 16^+$ transition. Both transitions are consistent with $L=2$ multipolarity.

TABLE III. The energies, spins, and parities of the excited states of $^{72}$Kr, and the energies, relative intensities, and measured multipolarities of transitions from these states.

| $E_x$ (keV) | $J^\pi$ ($\hbar$) | $E_\gamma$ (keV) | $I_\gamma$ (%) | $L$ ($\hbar$) |
|---|---|---|---|---|
| 710 | $2^+$ | 710.1(2) | ~200 | 2 |
| 1322 | $4^+$ | 611.8(2) | | 2 |
| 2114 | $6^+$ | 791.6(2) | | 2 |
| 3110 | $8^+$ | 995.5(2) | 100 | 2 |
| 3799 | | 1685(1) | <20 | |
| 4295 | $10^+$ | 1184.9(2) | 76(12) | 2 |
| 4758 | | 959.1(8) | <20 | |
| | | 1648(1) | <20 | |
| 5650 | $12^+$ | 1354.9(3) | 61(11) | 2 |
| 6050 | | 1292.0(8) | 41(12) | |
| 7159 | $14^+$ | 1509.2(3) | 65(12) | 2 |
| 7165 | | 1115.4(8) | 32(12) | |
| 8528 | $(16^+)$ | 1369.2(8) | 10(2) | |
| 8597 | | 1432.1(9) | 27(9) | |
| 8747 | $16^+$ | 1588.2(6) | 29(5) | 2 |
| 8821 | $16^+$ | 1661.9(6) | 22(3) | 2 |
| 9769 | $18^+$ | 1021.9(6) | 18(2) | 2 |
| | | 1240(1) | 10(2) | |
| 10 041 | | 1444.3(9) | 25(8) | |
| 10 560 | $18^+$ | 1738.6(6) | 15(2) | 2 |
| 11 236 | $20^+$ | 1466.7(8) | 20(3) | 2 |
| 11 537 | | 1495.8(9) | 22(6) | |
| 12 390 | $(20^+)$ | 1830(1) | 19(3) | |
| 13 136 | | 1599(1) | 18(6) | |
| 13 182 | $22^+$ | 1946(1) | 17(3) | 2 |
| 14 305 | $(22^+)$ | 1915(1) | 13(2) | |
| 14 915 | | 1779(1) | <10 | |
| 15 642 | $(24^+)$ | 2460(2) | 16(2) | |
| 16 339 | $(24^+)$ | 2034(1) | 11(2) | |
| 16 976 | | 2061(3) | <5 | |
| 18 476 | $(26^+)$ | 2137(2) | 5(1) | |
| | | 2834(3) | <5 | |
| (18 705) | $(28^+)$ | 3063(3) | 5(1) | |

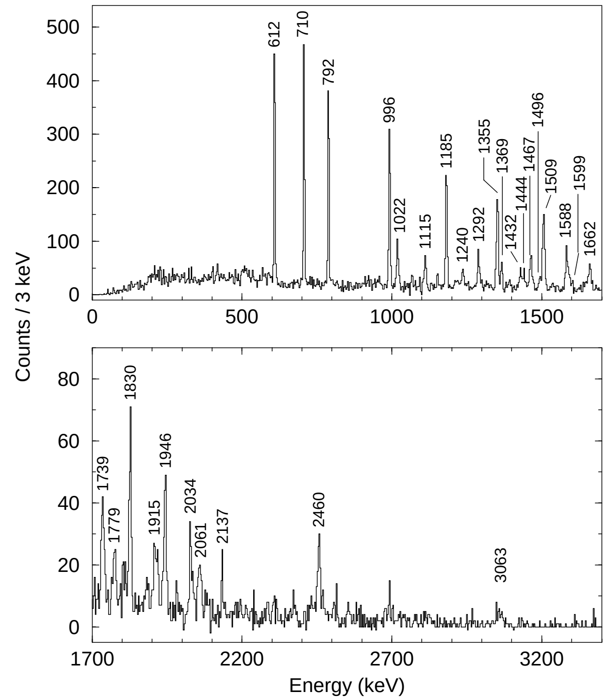


FIG. 5. A composite spectrum of $\gamma$-ray transitions in $^{72}$Kr. The spectrum was obtained by summing all possible channel-subtracted $\gamma\gamma$ gates associated with $^{72}$Kr produced in the $^{40}$Ca+$^{40}$Ca reaction.

The band crossing situation in $^{72}$Kr is indeed unusual: at spin $J=16$ the ground state band is crossed by a more favored configuration, but at higher spin, near $J=24$, the bands appear to cross once more.

## IV. DISCUSSION OF RESULTS FOR $N=Z$ NUCLEI

### A. $^{68}$Se

Several changes of the kinematic moment of inertia, $J^{(1)}$, as a function of the rotational frequency can be seen in Fig. 10. The new data for $^{68}$Se are compared with a recent study of $^{70}$Se [35]. It can be seen that there are quite striking similarities, which help with configuration assignments. At the lowest spins, collective oblate rotation (with a very low moment of inertia) is rapidly superseded by more favored near-prolate rotation [27]. In our original study, the next irregularity was interpreted as due to the alignment of $g_{9/2}$ particles in a near-prolate potential, despite the low gain in alignment. In the present work we have observed a much larger backbend above $J=14$. These effects, especially the dramatic high-spin backbend, were predicted by Sun [9] prior to the experiment, and were suggested to correspond to the subsequent 2-$qp$ and 4-$qp$ alignment of protons and neutrons. The agreement is not perfect, but is surprisingly good in a schematic model where the core has fixed deformation. The model does include configuration mixing, and, as predicted, the observed sharpness of the second irregularity indicates very little mixing between the crossing configurations. Wyss and Satula [6] have also predicted the high-spin behavior of $^{68}$Se, through an extended TRS calculation. They also find several shapes near the yrast line, with the oblate ground state ~0.5 MeV more bound than the lowest prolate configuration. In their model they find two excited bands, $d2$ which corresponds to a more collective core shape of $\beta_2$ ~0.33 and $\gamma=-18°$ (corresponding to a quadrupole moment of $Q_t=2.33$ $e$ b), and a less collective $d1$ configuration with $\beta_2=0.34$ and $\gamma=+32°$ (corresponding to $Q_t=1.21$ $e$ b). These bands have characteristics very similar to our new data. The first two irregularities in the moment of inertia correspond to changing from the oblate ground state to the initial prolate configuration, then to the collective $d2$ shape. In nature, the $d2$ configuration must lie slightly lower in excitation and the $d1$ configuration must lie higher than in the calculation, to get the sequence of crossings to match. The swooping fall of the moment of inertia at the highest spins is characteristic of a band moving towards termination and losing collectivity. In potential energy terms this is usu-

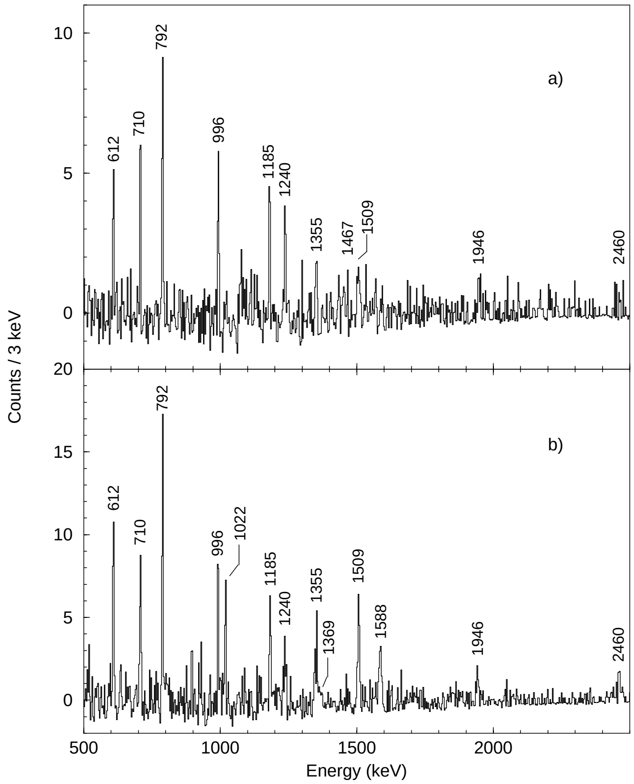


FIG. 6. Spectra for $^{72}$Kr obtained from sums of $\gamma\gamma$ gates. In the upper panel, one of the gates is the 1369 keV transition, and the other gate is a member of the ground state band below spin $14^+$. In the lower panel, one of the gates is the 1467 keV transition, and the other gate is a member of the ground state band below spin $14^+$. The 1240 keV transition from the 9769 keV, $18^+$ state appears in both spectra, but the 1022 keV→1588 keV cascade is seen only in coincidence with $\gamma\gamma$ gates that include the 1467 keV transition.

ally reflected in the minimum in the surface moving towards the noncollective, $\gamma = +60°$ axis of the $(\beta,\gamma)$ shape surface. An analysis of $^{68}$Se using the relativistic mean field approach and the cranked Nilsson-Strutinsky method [7] supports

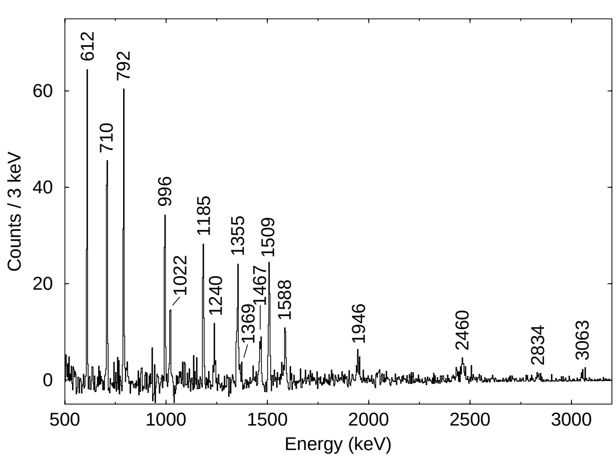


FIG. 7. A sum of $\gamma\gamma$ gates selected to enhance the transitions in band $A$ in $^{72}$Kr. One member of each pair of gates belongs to band $A$, and the other belongs to the ground state band.

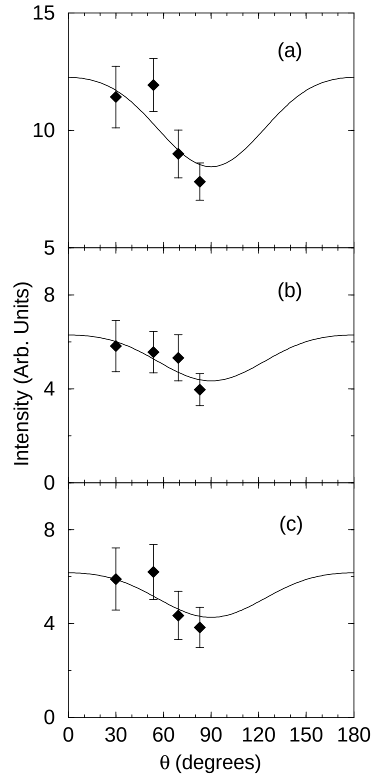


FIG. 8. Angular distribution data for the (a) 1588-keV, (b) 1662-keV, and (c) 1022-keV transitions in $^{72}$Kr. All transitions are consistent with $L=2$ multipolarity, and support the assignments of the three $J^{\pi}=16^+$ states in the "forking" region around 8700 keV.

these findings; that the yrast line has many changes in configurations, from collective oblate $(\beta_2=0.22, \gamma=-60°)$, to axial prolate $(\beta_2=0.22, \gamma\sim 0°)$, then collective triaxial $(\beta_2 =0.35, \gamma=-35°)$, and finally to a low-collectivity triaxial shape $(\beta_2=0.33, \gamma=+35°)$. The less collective high-spin configuration is of "[2,2]" nature, with two protons and two neutrons in the $g_{9/2}$ shell.

The complex Hartree-Fock-Bogoliubov calculations of Petrovici *et al.* [8] investigated oblate and prolate shapes in $^{68}$Se. Their approach is especially good for investigating the mixing of states and the variation of specific residual interactions. They infer considerable mixing of configurations at low spin, but find a great simplification with angular momentum. Above spin $J=10$ they predict the prolate and oblate bands to be rather pure, with transitional quadrupole moments $Q_t=2.33$ $e$ b for the prolate band and 1.91 $e$ b for the oblate band, results which are in reasonable agreement with the TRS calculations. It is interesting to note that the seminal work of Nazarewicz *et al.* [1] predicted this type of behavior to be generic to the region. Specifically, nearly 20 years ago they predicted bands with near-prolate deformation with smoothly increasing moments of inertia, and near-oblate noncollective coexisting bands with sharp jumps in moment of inertia at $J^{\pi}=8^+$ and $16^+$. In this picture the $^{68}$Se yrast line represents a change from collective oblate to prolate, then onwards towards noncollective oblate motion as the optimal mode of carrying angular momentum.

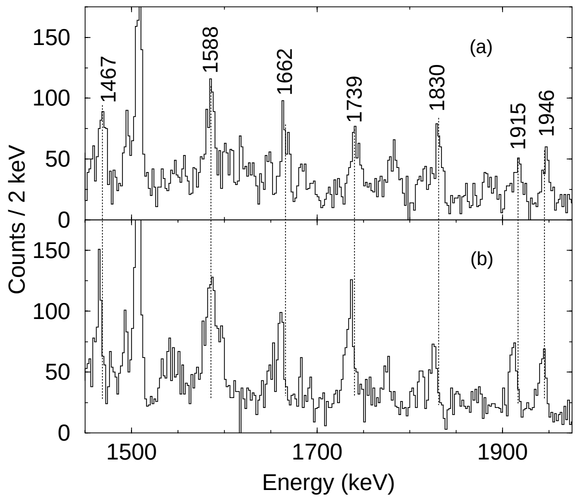


FIG. 9. A spectrum of $\gamma$ rays in coincidence with transitions in the ground state band of $^{72}$Kr. The upper panel shows the $\gamma$ rays detected at forward angles ($\theta<90°$), and the lower panel shows those detected at backward angles ($\theta>90°$). An event-by-event Doppler correction has been applied to the data, under the assumption that the $\gamma$ rays were emitted after the nucleus left the target. The correction is appropriate for the 1588-keV transition. Notice that the 1662-keV, 1739-keV, 1830-keV, and 1915-keV transitions of band $B$ are not correctly shifted, requiring a $\beta$ larger than the one applied, and indicating that the $\gamma$ rays were emitted while the recoiling nucleus was still in the target. The 1467- and 1946-keV transitions of band $A$ require smaller corrections to the recoil velocity.

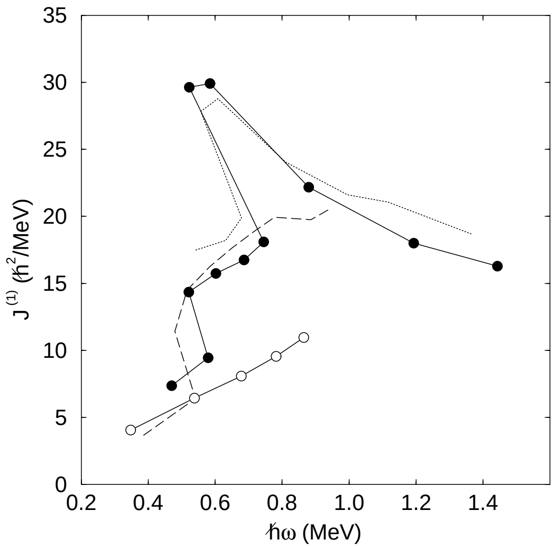


FIG. 10. The kinematic moments of inertia $J^{(1)}$ for $^{68}$Se (open and closed circles) and $^{70}$Se [35] (dotted and dashed lines). For $^{68}$Se, the open circles are the oblate ground state band $C$, and the closed circles are the bands $A$ and $B$. For $^{70}$Se, the dashed line is the ground state band, and the dotted line is the positive parity excited band labeled as $C$ in Ref. [35].

As we will see in the following section, two distinct bands are predicted, and seen, in $^{72}$Kr, corresponding to building angular momentum collectively with a near-prolate shape, or less collectively with a near-oblate shape. Both of these bands are also expected for $^{68}$Se. We have searched for the smoother collective sequence in our $^{68}$Se data. We were not able to find any candidate transitions for an extension of the ground state band above spin $J=14$. This was partially due to the size of the datasets, the krypton experiment having more than double the selenium statistics, but also due to the fact that in krypton the bands remain close together in excitation. Indeed, the bands in krypton cross twice, and so appear to have a rather equal population. The smooth continuation of the ground state band is non-yrast by less than 300 keV at $J=16$ and carries 22(3) units of relative intensity compared with the 29(5) units for the less-collective sequence at the same spin. In selenium, a smooth extension of the ground state band would place the more collective $J=16$ level nonyrast by greater than 500 keV. Experimentally, its nonobservation implies it carries less than 25% of the flux relative to the observed high-spin band.

### B. $^{72}$Kr

As in $^{68}$Se, the moment of inertia is very irregular and the yrast line has many changes in structure. Figure 11 shows the kinematic moments of inertia of bands in $^{72}$Kr. The oblate-prolate competition near the ground state is less evident in $^{72}$Kr than in $^{68}$Se as the transition to prolate states is almost immediate. At low spin only one sequence of $\gamma$-decaying states is known, although a low-lying $J^{\pi}=0^{+}$ isomer, presumably the prolate bandhead, has been recently identified [36,37]. The ground state band from $J\sim4$ to $J=14$ reflects the rotation of a near-axial prolate shape [10]. Above $J=14$ three modes of carrying angular momentum appear to be supported, all of which are energetically favored at some spin. One mode involves maintaining the core deformation, and the high collectivity. This is band $B$ in Fig. 1 (right panel) and appears to most closely correspond to a continuation of the ground state sequence. It is marked as * in Fig. 11, where it can be seen that a rather gradual change in structure occurs at high spin. As this is an $N=Z$ nucleus, protons and neutrons should align at near-identical frequencies, so the gain in alignment should be large.

A second mode of rotation involves a sharply reduced core deformation, polarized by aligned $g_{9/2}$ protons and neutrons. The reduction in collectivity is consistent with our measurement of differential Doppler shifts (Sec. III B) and from calculation [10]. This is the sequence marked "$A$" in Fig. 1. For some spin range between $J=18$ and $J=24$, it is the energetically favored mode, with a large gain in spin from the aligned particles. However, the reduced collectivity of the core and its smaller moment of inertia means that with increased rotation this band slowly loses out energetically compared to the ground state sequence, and becomes nonyrast again above spin $J=24$. Near the second crossing point, the $J=26$ states in sequences $A$ and $B$ are nearly degenerate, and some configuration mixing does appear to occur, as evidenced by the tentative interband transition of 2834 keV. Phase space considerations alone would make this out-of-band path the dominant decay branch from the 18 476-keV state, four times stronger than the in-band decay. In fact, it is a $<30\%$ branch. This order of magnitude reduc-

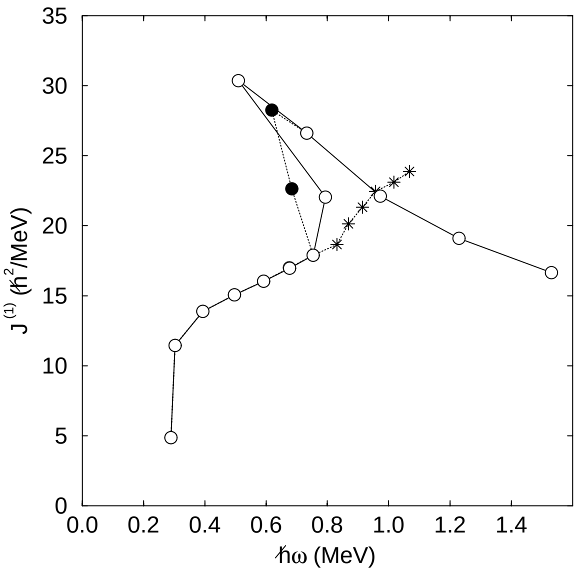


FIG. 11. The kinematic moments of inertia $J^{(1)}$ as a function of the rotational frequency $\hbar\omega$ for bands *A* and *B* of $^{72}$Kr. The ground state band forks into three branches above $\hbar\omega\sim 0.75$ MeV, with the open circles representing band *A*, the asterisks (*) band *B*, and the closed circles showing the 1240 keV → 1369 keV cascade from the $18^+$ level at 9769 keV.

tion indicates a small overlap of wave functions in the two sequences with rather little mixing, despite the $J^{\pi}=26^+$ states being separated by only 230 keV.

Finally, there is a third $J=16$ state at 8528 keV which does not support any observable rotational band, although it is the yrast $J=16$ configuration. From its sharp line shape in the study of de Angelis *et al.* [10], it appears to be relatively long lived, and possibly corresponds to a near-spherical fully aligned $(g_{9/2})^4$ shell model state. To have the least collective state as part of the yrast line is very unusual. It appears to be similar to the situation in $^{24}$Mg [38] where a favored non-collective $J=8$, $(d_{5/2})^4$ configuration is substantially more bound than the collective rotational bands.

## V. COMPARISON TO NEIGHBORING EVEN-EVEN NUCLEI

In analysis of rotational spectra it is sometimes convenient to define a fixed core moment of inertia, then study relative changes in spin (usually denoted *i*, the relative alignment) and changes in energy (usually denoted *e*, the Routhian) with respect to the fixed core. This approach is quantitatively powerful in rigid fixed-shape nuclei, like those found in the center of the rare-earth and actinide nuclei.

Bengtsson and Frauendorf [39] have presented clear prescriptions for extracting alignments, Routhians, and crossing frequencies from experimental data. Specifically, for true backbending, the crossing frequency is the point at which the Routhian loops and crosses itself. For stronger interacting upbends, the straight sections of the Routhian curves need to be extrapolated back to a crossing point. In this framework, the concept of an *S* band is clear-cut; it is associated with the alignment of a single pair of particles without any perturbation of the core. Because it has a great deal of overlap with the ground state band, this two-quasiparticle excitation can be accurately calculated, as can the frequency at which it becomes yrast. By comparison of odd- and even-nuclei with the Bengtsson and Frauendorf cranked shell model, Garrett *et al.* [40] were able to investigate normal $T=1$ pairing in detail and study the reduction of pairing due to blocking of orbits. They were also able to infer that the pairing interaction had higher multipole, specifically quadrupole, components. However, their approach relied on stable deformation of the nuclei to infer shifts in crossing frequency. This platform appears essential for the unambiguous use of rotational behavior in investigating pairing correlations.

In the $A\sim 70$ region the condition of shape stability is manifestly not met. The dramatic band crossings are *not* the mere alignment of pairs of particles to form an *S* band. They represent the crossing of totally different bands with unrelated structure. Estimating the crossing frequency of different structures involves calculation of the absolute binding energy and moment of inertia of each configuration, and not just the incremental changes due to breaking of an individual pair of particles. At present, the required level of accuracy for such a calculation is beyond the scope of current theory which is needed to gain quantitative information on $np$ pairing.

For the purpose of discussion and comparison we have calculated the Routhians for $^{68,70}$Se and $^{72,74}$Kr using the reference moment of inertia $J_o=17.5\hbar^2$/MeV taken from the work of de Angelis *et al.* [10] with an $A^{5/3}$ mass scaling. The new data for $^{70}$Se are from Rainovski *et al.* [35] and for $^{74}$Kr from Rudolph *et al.* [41]. The reference is only for relative portrayal of the data, removing the bulk average energy of rotation, and does not reflect any assumption about the nuclei having the same shape. Figure 12 shows these Routhians. It is very clear that all these nuclei have features in common. At high spin all but $^{68}$Se have been found to have two close-lying, even spin positive parity bands, an unusual feature in itself. One of the bands always has a very sharp backbend. Theoretical calculations [6,35] for $^{68,70}$Se indicate that this feature is associated with the alignment of $g_{9/2}$ protons and neutrons in a low-collectivity near-oblate potential (i.e., the triaxiality is large and positive in the Lund convention). The predicted shapes in both nuclei are in good agreement, $(\beta,\gamma)$ of $(0.34,+32°)$ [6] and $(0.35,+35°)$ [7] for $^{68}$Se, and $(0.30,+24°)$ for $^{70}$Se [35]. Experimentally, for $^{70}$Se, this prediction is reinforced by the unusual property of the recently studied [42–44] oblate, $\beta$-decaying, $J^{\pi}=9^+$ isomer in $^{70}$Br that exclusively picks out this nonyrast structure and shows no decay branch to the more collective ground state sequence that is favored by phase space. The second band has a much smoother behavior. Calculations indicate this to correspond to states in a distinct second minimum of the potential energy surface that has a similar quadrupole deformation but has a negative triaxiality parameter $\gamma$ in the Lund convention, which leads to higher collectivity and a larger moment of inertia. Again the calculated minima agree quite well: $(\beta,\gamma)$ of $(0.33,-18°)$ [6] and $(0.33,-35°)$ [7] for $^{68}$Se, and $(0.35,-45°)$ for $^{70}$Se [35].

$^{72}$Kr seems to follow the behavior of the selenium isotopes rather closely, as can be seen from the Routhians of

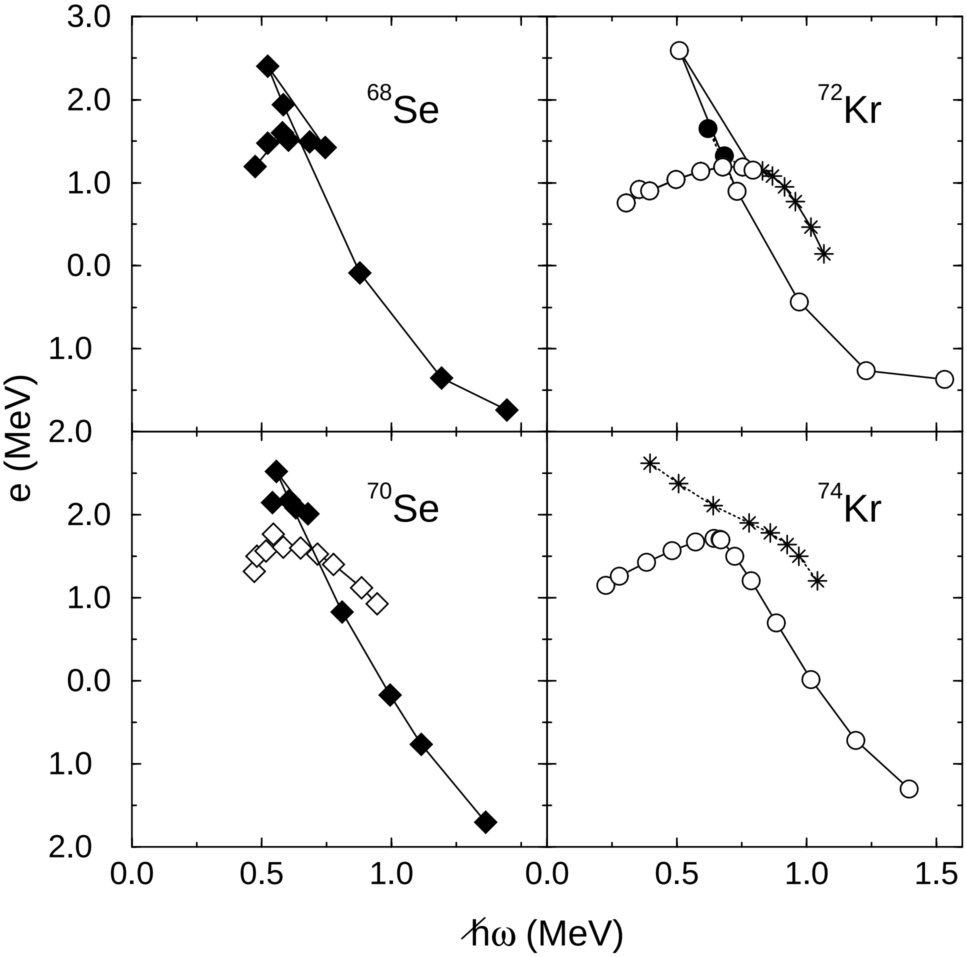


FIG. 12. The experimental Routhians $e$ for $^{68,70}$Se and $^{72,74}$Kr calculated using a reference of $17.5\hbar^2$/MeV from Ref. [10] and a $A^{5/3}$ scaling for the other nuclei.

Fig. 12. As discussed in Sec. III B, the lifetimes measured in this work appear to follow the selenium predictions of two stable minima associated with more and less collective bands. This similarity is borne out by a calculation of transitional quadrupole moments. Taking the topology predicted [6] for $^{68}$Se the two configurations have $Q_t = 2.33$ and 1.21 $e$ b, respectively. Rescaling these moments for the slightly different $A$ and $Z$ of $^{72}$Kr would suggest moments of $Q_t = 2.51$ and 1.30 $e$ b for the krypton bands. This is in remarkably good agreement with our differential lifetime results of $Q_t = 2.52(47)$ and 1.15(15) $e$ b. A more direct comparison with earlier calculations [10] of $^{72}$Kr that predicted minima of higher deformation (collective band with $\beta_2 = 0.43$, $\gamma = -22°$, less-collective band with $\beta_2 = 0.30, \gamma = +10°$) shows poorer agreement, with $Q_t = 3.39$ $e$ b and 1.90 $e$ b for the more and less collective bands.

There are also differences between these nuclei which should be noted. The most striking of these is that the structures in the $N = Z$ nuclei appear to evolve quite separately, with few crossing transitions between bands, whereas the $N = Z + 2$ nuclei show many linking transitions over a wide range of spin. As the basic configurations are very different, these linking transitions probably reflect a varying degree of mixing between the states at each spin. $^{74}$Kr shows the most mixing. In that case the two bands seem to cross adiabatically at $J \sim 14$, and the nature of yrast and yrare excitations are smoothly exchanged. Analysis of the branching ratios of the intraband to interband transitions is revealing. When the $E_\gamma^5$ phase space factor is removed, and using two-level mixing assuming the crossing transitions arise solely from mixing of the wave functions, one finds that the $J = 14$ states are almost completely mixed, whereas all the other crossing delays have quite small ($< 10\%$) mixtures. Thus, the yrast sequence starts at $J = 4$ in the collective minima and ends at $J > 18$ in the less collective one. This provides an alternate and self-consistent explanation for the experimentally observed fall in transitional quadrupole moment [1] from $Q_t = 2.8$ $e$ b to 2.1 $e$ b, although the authors of that work originally interpreted the effect as due to a single shape with its axial quadrupole deformation shrinking from $\beta_2$ of 0.36 to 0.28. The different degrees of mixing can provide information about the barrier between configurations. It appears that the $N = Z$ nuclei have deeper, better defined minima, as the shapes where shell gaps cause extra binding are optimized simultaneously for protons and neutrons. It is likely that $^{74}$Kr has minima that are closer in shape, separated by a lower barrier, and thus has more mixing. Indeed, the lifetime measurements on $^{72}$Kr from this work show a bigger fractional difference in collectivity compared to the difference measured for $^{74}$Kr. An alternative interpretation of the yrare band in $^{74}$Kr has been suggested [41] involving neutron alignment in a prolate potential. However, in light of the new data and the close similarity of $^{72,74}$Kr, we feel that the shape mixing explanation offers a more consistent picture for these bands. The "two-shape" explanation may also resolve the long standing puzzle of the degree of alignment $i$ in $^{74}$Kr. Although the upbend is always described as a $(g_{9/2})^4$ alignment, $i$ is found to be approximately $8\hbar$, as opposed to the $16\hbar$ that is expected for a straightforward cranked shell model interpretation [39].

## VI. BAND CROSSINGS AND THE SEARCH FOR ALIGNMENT DELAYS

With this two-shape scenario in mind we can now address the issue of band crossings and alignment delays in more detail. In a situation where the nuclei have two coexisting shapes, several different types of crossings can occur. In each minimum, particle alignment will proceed and cause traditional $S$-band type crossings. For the $N=Z$ nuclei these crossings should occur simultaneously for protons and neutrons. Further, as the two minima are associated with different moments of inertia, the minima themselves can have an additional crossing as the rotational frequency changes to favor one shape over another. For $^{68,70}$Se, the less- and more-collective sequences have crossings at $\hbar\omega=0.65(2)$ and $0.70(2)$ MeV, respectively. Thus the crossing frequency is lower in the $N=Z$ case compared to $N=Z+2$, contrary to any expectations of a delay. However, this is a crossing of shapes, and not the type of crossing that would use to seek $np$ correlations, for which one needs stable deformation. In $^{70}$Se the collective sequence shows such strong interaction between configurations that the alignment of $g_{9/2}$ particles cannot be discerned at all. Consequently, no statement can be made about the crossing frequency in the collective configuration. For $^{68}$Se, the collective sequence could not be found at high spin, and as a result, can provide no additional information.

The krypton isotopes are more informative. The crossing between collective and noncollective structures is now clear, especially in $^{72}$Kr, and both lie close to $\hbar\omega=0.67(2)$ MeV, perhaps with a very small extra delay for the $N=Z$ isotope, but if so the delay is $<0.01$ MeV. The delay reported by de Angelis [10] is now revealed as an artifact arising from the sharpness of the backbend; only when the full sequence is mapped out can the actual crossing frequency be determined. The new experimental crossing frequency is somewhat higher than the TRS calculation reported in Ref. [10], where a crossing of $\hbar\omega=0.55$ MeV was predicted in a calculation that did not include $np$ pairing. To obtain this result it was necessary to calculate the shapes of the bands independently as well as the difference in their binding energies. The predicted shapes do not quite match the quadrupole moments extracted from our lifetime estimates, and this difference could account for the discrepancy in crossing frequency between theory and experiment.

For both $^{72,74}$Kr the more collective bands extend well past the shape crossing, and then show evidence for another irregularity. It is this second crossing that most closely resembles the normal notion of alignment in a fixed shape potential. Although the $S$-band interaction in the higher frequency region is strong, one can extract a crossing frequency of $\hbar\omega\sim0.88(3)$ for both $^{72,74}$Kr, despite the fact that the strong shape mixing in $^{74}$Kr somewhat masks this crossing. Thus, even when a crossing of the appropriate type is located there seems little evidence for any alignment delay. In theoretical calculations [16–19] considerable emphasis has been put on the fact that the $N=Z$ nuclei are especially susceptible to enhanced $T=0$ correlations, and that the effects should fall away very rapidly in $N=Z+2,Z+4$ nuclei. The data presented here do not seem to support any suggestion that the crossings in $N=Z$ nuclei occur at drastically different frequency when compared to $N=Z+2$ nuclei, and thus do not obviously provide any clear evidence for $T=0$ correlations. However, it should be noted that this crossing frequency, $\hbar\omega=0.88(3)$ MeV, is extremely high. A detailed analysis [12] using the cranking model with reasonable deformations, consistent with our lifetimes, and normal $T=1$ pairing could not reproduce the high crossing frequency. We have performed similar calculations and reached the same conclusion. Only when $T=1$ and $T=0$ pairing correlations were included [12] could the experimental situation be approached. Thus, although the bands and their crossings are now clearer and show no evidence for a delay between $N=Z$ and $N=Z+2$ nuclei, the apparent $S$-band crossing in the collective sequence is difficult to reconcile with the "normal" cranking analysis.

It is interesting to follow the progression of the minima in the potential energy surface of $N=Z$ nuclei with increasing mass. This pattern is shown in Fig. 13. For selenium, the highest spin states are dominated by the low-collectivity near-oblate configuration, while for krypton, a close balance is reached and both low- and high-collectivity configurations coexist. Only for strontium and heavier nuclei, the strong influence of the $N,Z=38,40$ prolate shell gaps dominates all structures and the near-prolate, high collectivity bands dominate. In the heavier $N=Z$ Sr, Zr, Mo, and Ru nuclei alignment delays or delay limits have been reported [13,14]. However, in the light of this work the decay schemes of these nuclei need to be developed to substantially higher spin before any firm conclusion can be reached concerning alignment delays.

## VII. CONCLUSION

We have extended the decay schemes of $^{68}$Se and $^{72}$Kr. The new data, when compared to each other and to neighboring nuclei, clarify considerably the band structure and the nature of the crossings. In $^{68}$Se, the yrast line shows many shape changes, from oblate to prolate, then collective triaxial, and finally noncollective oblate. $^{72}$Kr exhibits a similar variety of shapes, but here the shapes coexist without much mixing. This variety of shapes allows a bewildering variety of possible particle alignments and backbends, both due to pair breaking associated with a single shape, and due to dif-

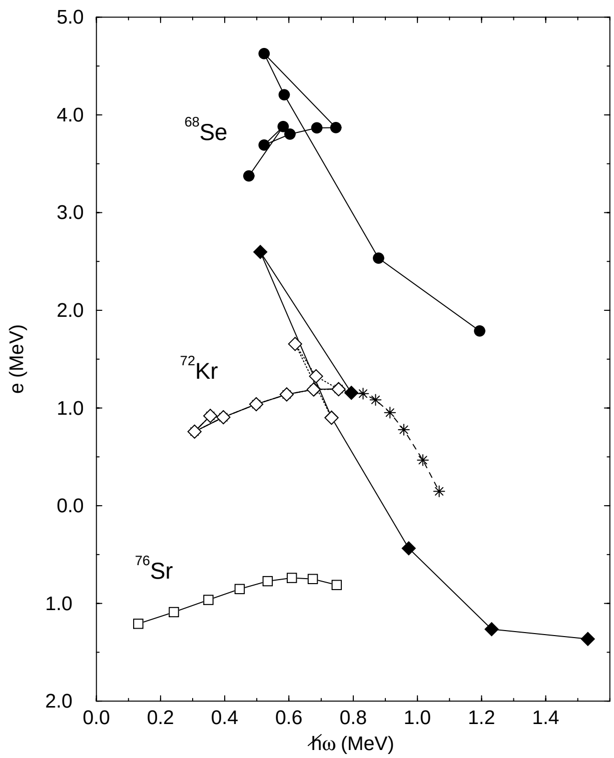


FIG. 13. The progression of Routhians for $N=Z=34$, 36, and 38 shown plotted using a reference scaled from the reference in Ref. [10]. The Routhians for the three nuclei have been offset relative to each other for clarity. It is interesting to note that the less collective, near oblate structure becomes less significant as the dominant prolate shell gap as $N=Z=38$ is approached.

ferent shapes crossing each other. Some of these crossings have been identified. The original report of a large alignment delay [14] in $^{72}$Kr, possibly due to $np$ pairing, arose from mistakenly comparing different types of crossings in $^{72,74}$Kr. Our differential Doppler shift measurements have helped categorize the bands. In this work, the bands have been carefully matched and the same crossings have been isolated in the two nuclei. No clear evidence for any relative delay can be found. Thus, we do not seem to have any evidence for $T=0$ $np$-pairing correlations, although the crossing frequency seems anomalously high. In the future, for more detailed investigation of the evolution of these bands, it must be demonstrated that the core shapes can be tracked through state-by-state lifetime measurements before any inferences about pairing can be drawn. The pairing field also influences the strength of interaction between configurations, and it may be that a careful investigation of the mixing between configurations in the crossing regions can provide a useful tool for probing the nature of the pairing correlations at high spin.

## ACKNOWLEDGMENTS

We would like to acknowledge a great deal of help in these studies. First, thanks should go to the scientists, support staff, and accelerator operators at the 88-Inch Cyclotron at Berkeley and the ATLAS accelerator at Argonne. We would especially like to thank Demetrios Sarantites for his help with the Microball, Yang Sun for providing calculations prior to publication and for many interesting and excellent theoretical discussions, Cyrus Baktash for pointing out to us the similarity between krypton isotopes, and Mike Carpenter for performing cranking calculations. The research was supported by the U.S. Department of Energy, particularly from Contract Nos. W-31-109-ENG-38 and FG02-94ER40834, which allowed the operation of Gammasphere at Argonne and Berkeley, and from the National Science Foundation Grant No. NSF PHY95-14157. S.M.F. acknowledges support from Research Corporation.

[1] W. Nazarewicz, J. Dudek, R. Bengtsson, T. Bengtsson, and I. Ragnarsson, Nucl. Phys. **A435**, 397 (1985).
[2] K. Kaneko and J.Y. Zhang, Phys. Rev. C **57**, 1732 (1998).
[3] S. Frauendorf and J.A. Sheikh, Phys. Rev. C **59**, 1400 (1999).
[4] Yang Sun and Javid A. Sheikh, Phys. Rev. C **64**, 031302(R) (2001).
[5] A.L. Goodman, Phys. Rev. C **63**, 044325 (2001).
[6] Ramon A. Wyss and Wojciech Satula, Acta Phys. Pol. B **32**, 2457 (2001).
[7] A.V. Afanasjev and P. Ring, Phys. Scr. **T88**, 10 (2000); Acta Phys. Pol. B **32**, 2469 (2001); (private communication).
[8] A. Petrovici, K.W. Schmidt, and A. Faessler, Nucl. Phys. **A710**, 246 (2002); **A704**, 144c (2002).
[9] Y. Sun, in Proceedings of the Conference on Nuclear Structure with Large Gamma-Arrays: Status and Perspectives, Legnaro, Italy, 2002, edited by G. de Angelis (Eur. Phys. J, in press); (private communication).
[10] G. de Angelis *et al.*, Phys. Lett. B **415**, 217 (1997).
[11] S.M. Fischer *et al.*, Nucl. Phys. **A682**, 35c (2001).
[12] N.S. Kelsall *et al.*, Phys. Rev. C **64**, 024309 (2001).
[13] N. Marginean *et al.*, Phys. Rev. C **63**, 031303(R) (2001).
[14] S.M. Fischer *et al.*, Phys. Rev. Lett. **87**, 132501 (2001).
[15] N. S. Kelsall *et al.*, in *Proceedings of the Conference on Frontiers of Nuclear Structure 2002, Berkeley, California, 2002*, edited by P. Fallon (Springer-Verlag, New Jersey, 2003).
[16] H.H. Wouter, A. Faeassler, and P.U. Sauer, Phys. Lett. **31B**, 516 (1970).
[17] A.L. Goodman, Adv. Nucl. Phys. **11**, 263 (1979); Phys. Rev. C **58**, R3051 (1998); **60**, 014311 (1999).
[18] A.W. Mountford, J. Billowes, W. Gelletley, H.G. Price, and D.D. Warner, Phys. Lett. B **279**, 228 (1992).
[19] O. Civitarese and M. Reboiro, Phys. Rev. C **56**, 1179 (1997).
[20] D.R. Bes, R.A. Broglia, O. Hansen, and O. Nathan, Phys. Rep. **34**, 1 (1977).
[21] P. Vogel, Nucl. Phys. **A662**, 148 (2000).
[22] A.O. Macchiavelli *et al.*, Phys. Rev. C **61**, 041303(R) (2000).
[23] R.R. Chasman, Phys. Lett. B **524**, 81 (2002); **555**, 204 (2003).
[24] I.Y. Lee *et al.*, Nucl. Phys. **A520**, 641c (1990).
[25] D.G. Sarantites, P.-F. Hua, M. Devlin, L.G. Sobotka, J. Elson, J.T. Hood, D.R. LaFosse, J.E. Sarantites, and M.R. Maier,

Nucl. Instrum. Methods Phys. Res. A **381**, 418 (1996).
[26] C.N. Davids, B.B. Back, K. Bindra, D.J. Henderson, W. Kutschera, T. Lauritsen, Y. Nagame, P. Sugathan, A.V. Ramayya, and W.B. Walters, Nucl. Instrum. Methods Phys. Res. B **70**, 358 (1992).
[27] S.M. Fischer, D.P. Balamuth, P.A. Hausladen, C.J. Lister, M.P. Carpenter, D. Seweryniak, and J. Schwartz, Phys. Rev. Lett. **84**, 4064 (2000).
[28] C.J. Lister, P.J. Ennis, A.A. Chishti, B.J. Varley, W. Gelletly, H.G. Price, and A.N. James, Phys. Rev. C **42**, R1191 (1990).
[29] S. Skoda *et al.*, Phys. Rev. C **58**, R5 (1998).
[30] B.J. Varley, M. Campbell, A.A. Chishti, W. Gelletly, L. Goettig, C.J. Lister, A.N. James, and O. Skeppstedt, Phys. Lett. B **194**, 463 (1987).
[31] H. Dejbakhsh *et al.*, Phys. Lett. B **249**, 195 (1990).
[32] P. A. Hausladen, Ph.D. thesis, University of Pennsylvania, 1998.
[33] J. F. Ziegler, *The Stopping and Ranges of Ions in Matter* (Pergamon, New York, 1980).
[34] A. Algora *et al.*, Phys. Rev. C **61**, 031303(R) (2000).
[35] G. Rainovski *et al.*, J. Phys. G **28**, 2617 (2002).
[36] W. Korten, Acta Phys. Pol. B **32**, 729 (2001).
[37] E. Bouchez *et al.*, Phys. Rev. Lett. **90**, 082502 (2003).
[38] D. Branford, M.J. Spooner, and I.F. Wright, Part. Nuclei **4**, 231 (1972).
[39] R. Bengtsson and S. Frauendorf, Nucl. Phys. **A314**, 27 (1979); **A327**, 139 (1979).
[40] J.D. Garrett *et al.*, Phys. Lett. **118B**, 297 (1982).
[41] D. Rudolph *et al.*, Phys. Rev. C **56**, 98 (1997).
[42] J. Döring *et al.*, in *Selected Topics in $N=Z$ Nuclei—Pingst 2000, Lund, Sweden, 2001*, edited by D. Rudolph and M. Hellstrom (University of Lund, Sweden, 2000), p. 131.
[43] A. Piechaczek *et al.*, Phys. Rev. C **62**, 054317 (2000).
[44] D.G. Jenkins *et al.*, Phys. Rev. C **65**, 064307 (2002).